DOI 10.5012/bkcs.2010.31.04.925

Visible-photoresponsive Nitrogen-Doped Mesoporous TiO_2 Films for Photoelectrochemical Cells

Jae Young Bae, Tae Kwan Yun,[†] Kwang-Soon Ahn,[†,*] and Jae-Hong Kim[†,*]

Department of Chemistry, Keimyung University, Daegu 704-701, Korea
[†]School of Display and Chemical Engineering, Yeungnam University, Gyeongsan, Gyeongbuk 712-749, Korea
[*]E-mail: jaehkim@ynu.ac.kr(JHK)
Received December 15, 2009, Accepted February 16, 2010

Nitrogen-doped TiO_2 (TiO_2:N) nano-particles with a pure anatase crystalline structure were successfully synthesized through the hydrolysis of $TiCl_4$ in an ammonia aqueous solution. The samples were characterized using X-ray diffraction (XRD), transmission electron microscopy (TEM), N_2-sorption, and UV-vis diffuse reflectance spectra (UV-vis DRS) techniques. The absorption edge of nitrogen-doped TiO_2 shifted into the visible wavelength region. The photoelectrochemical (PEC) performances were investigated for the TiO_2 mesoporous electrodes doped with different nitrogen concentrations. The TiO_2:N electrodes exhibited much higher PEC responses compared to the pure TiO_2 electrode because of the significantly enhanced visible-photoresponsibility of the TiO_2:N electrodes.

Key Words: Nitrogen-doped TiO_2, Visible-photoresponsive, Photoelectrochemical cells, Mesoporous electrodes

Introduction

Titanium dioxide (TiO_2) has attracted considerable interest for use as a photoelectrode in photoelectrochemical (PEC) cells such as PEC water-splitting cells and dye-sensitized solar cells because of it relatively low cost, non-toxicity, and long-term stability against corrosion.[1-3] However, TiO_2 has a wide band gap (3.2 eV for anatase and 3.0 eV for rutile),[4] which allows it to absorb ultraviolet light (~4% of solar energy) and be transparent for most solar irradiation.[5] Many groups have investigated methods to enhance its photoactivity under visible light illumination. Impurity doping is one of the typical approaches for extending the spectral response of titania into the visible light region. These doping techniques can either substitute other metals, such as Fe[6], Ni[7], and Cr[8], *etc*., into a Ti site or nonmetals, such as B[9], C[10], N[11], and F[12], in order to efficiently extend the photo-response from the UV region to the visible light region. The simplest and most feasible TiO_2 modification approach for achieving visible-light-driven PEC systems seems to be nitrogen-doping.

As early as 1986, Sato[13] reported that the calcination of NH_4Cl or NH_4OH with titanium hydroxide caused the photocatalyic sensitization of TiO_2 into the visible light region due to the NO_x impurity. Later studies showed that TiO_2 could be doped with nitrogen using various physical and chemical methods.[14-17] The traditional synthetic method of nitrogen-doped TiO_2 was followed by calcining TiO_2 in an ammonia atmosphere at high temperature. In addition to the energy waste caused by heating the sample, the treatment under high temperature usually induces particle agglomeration, leading to decreased surface area.[18]

In this study, nitrogen-doped anatase TiO_2 was successfully synthesized using a wet method, i.e., a hydrolysis process, which did not need a high calcination temperature. Nitrogen-doped TiO_2 was prepared through the simple addition of ammonia water to an aqueous solution, and exhibited a good photoactivity in the visible light region, a good crystallinity, and a high BET specific surface area. TiO_2 photoelectrodes with various concentrations of nitrogen were tested for H_2 water-splitting in order to confirm the effect of nitrogen doping on the PEC activity of prepared TiO_2. These results proved that the nitrogen-doped TiO_2 electrodes can potentially be beneficial to PEC cells in the visible light region.

Experimental Section

Preparation of nitrogen-doped TiO_2 particles. Titanium tetrachloride (99.9%, $TiCl_4$) was used as the main starting material and was used without any further purification. $TiCl_4$ was dissolved in doubly distilled water (0.7 mol/L) in an ice-water bath. This aqueous solution was then mixed with $(NH_4)_2SO_4$ (for preparation of anatase phase) in a temperature-controlled bath with continuous stirring at 90 °C for 24 h. Subsequently, ammonia water was added to prepare nitrogen-doped TiO_2. Three different mole ratios of ammonia to $TiCl_4$ (i.e., N/Ti) of 10, 15, and 20 were used. After continuous stirring for 6h, the precipitated TiO_2 was separated from the solution by using centrifugation and repeatedly washed with distilled water. The hydrous TiO_2 was dried at 80 °C under vacuum and grind into a fine powder. Then the samples were calcined at 400 °C for 3 h. For comparison, pure TiO_2 nanoparticles (N/Ti = 0) were synthesized using the same technique without the addition of ammonia water.

Materials characterization. The powder XRD patterns were collected using a powder diffractometer (PANalytical X'pert PRO MRD) with Cu Kα radiation (40 kV, 25 mA) at step size of 0.02°/s over a range from $20^o < 2\theta < 80^o$. The samples were prepared as thin layers on metal slides. For the TEM observations, powder specimens were preground, deposited onto a grid with a holey carbon film, and then rapidly transferred to a transmission electron microscope (Hitach H-7100) with an accelerating

voltage of 120 kV. The N_2-adsorption isotherms were measured at 77 K on a nitrogen adsorption apparatus (Quantachrome QUADRASORB SI). The volume of adsorbed N_2 was normalized using standard temperature and pressure. Prior to the experiments, the samples were dehydrated at 200 °C for 2 h. The specific surface area was determined from the linear portion of the BET equation (P/P_0 = 0.05 - 0.30). The UV-vis diffuse reflectance spectra were obtained from dry-pressed disk samples using a UV-vis-NIR spectrophotometer (Varian Cary 100) that was equipped with an integrating sphere assembly, with $BaSO_4$ as the reflectance sample.

Fabrication and measurement of PEC photoelectrode. The PEC measurements were performed in a three-electrode cell with a flat quartz window to facilitate the illumination of the photoelectrode surface. The mesoporous TiO_2:N films (active area: 0.25 cm^2) were used as the working electrodes. A Pt sheet and a Ag/AgCl electrode (with saturated KCl) were used as the counter and reference electrodes, respectively, with a 1 M KOH basic aqueous solution as the electrolyte. The PEC response was measured using a photodiode power meter and a Xe lamp (150 W) with a light intensity of 100 mW/cm^2. The photocurrent-voltage performances were measured under chopped light on/off illumination during a potential sweep (scan rate: 5 mV/s). The PEC performance of Degussa P25 TiO_2 which consists of anatase and rutile phases was also investigated with comparison to that of synthesized TiO_2.

Results and Discussion

Crystalline structure of nitrogen-doped TiO_2. Nitrogen-doped TiO_2 (TiO_2:N) nanoparticles were synthesized by the hydrolysis of $TiCl_4$ in an ammonia aqueous solution. Figure 1 shows the XRD results that were used to investigate the crystalline structure of the samples. The patterns of all the samples were indexed to only the anatase phase of TiO_2 (JCPDS 21-1272). Therefore, the anatase phase was retained without phase change after nitrogen doping.

The crystallite sizes of the samples were calculated by applying the Debye-Scherrer formula[22] in Equation (1) to the anatase (101) diffraction peaks:

$$L = K\lambda / \beta\cos\theta, \quad (1)$$

In this equation, L is the crystallite size in angstroms, K is a constant equal to 0.89 for this study, λ is the wavelength of the X-ray radiation (Cu Kα = 0.15406 nm), β is the corrected band broadening after the subtraction of the equipment broadening, and θ is the diffraction angle. The values of the crystallite sizes are provided in Table 1 along with other physical properties.

Some of the structural characteristics of pure TiO_2 and nitrogen-doped TiO_2 are shown in Table 1. The crystallite size slightly increased after nitrogen doping. In a typical wet process, the TiO_2 materials were synthesized through the competition between the nucleation and the growth. In the strong acidic environment generated by the hydrolysis of $TiCl_4$, the nucleation and the growth of TiO_2 clusters were both at intermediate rates. After adding the ammonia solution, the growth rate accelerated and the nucleation and the growth were no longer at equilibrium.[19] Additionally, the "*d*" space values did not change, implying that, the nitrogen was introduced into the lattice of the nitrogen-doped samples without changing the average unit cell dimension. The BET surface area of nitrogen-doped TiO_2 was larger than pure TiO_2 because the nitrogen doping had a stabilizing effect on the colloidal particles, which inhibited particle agglomeration.[20]

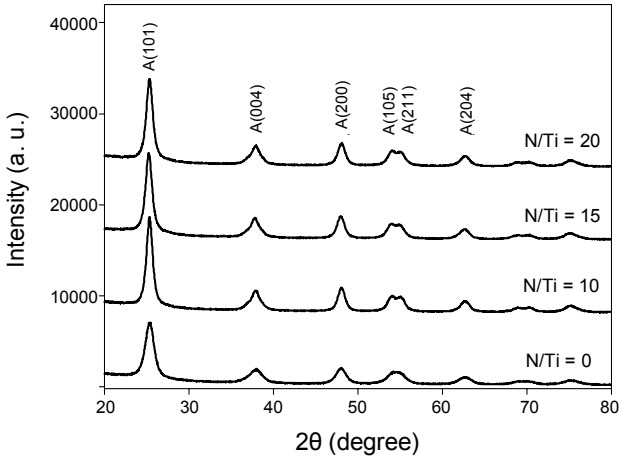

Figure 1. XRD patterns of nitrogen-doped TiO_2 with various N/Ti ratios.

Table 1. Physical properties of pure TiO_2 and nitrogen-doped TiO_2

Sample	Crystallite size (nm)	d spacing (Å)	BET (m^2/g)
N/Ti = 0	7.3	3.51	166
N/Ti = 10	10.6	3.51	173
N/Ti = 15	9.8	3.52	176
N/Ti = 20	9.9	3.51	203

Morphology of nitrogen-doped TiO_2. The morphology of the pure TiO_2 and nitrogen-doped TiO_2 powders were investigated using the TEM images in Figure 2. The images (Figure 2a and b) revealed that the pure TiO_2 and nitrogen-doped TiO_2 (N/Ti = 15) samples consisted of agglomerates of the primary particles with average diameters of 7 - 10 nm, which were in agreement with the crystallite sizes calculated from the XRD patterns.

Photo-absorption and PEC properties. Usually, nitrogen doping has an obvious effect on the light absorption characteristics of TiO_2. Figure 3 shows the diffuse reflectance spectra of pure TiO_2 and nitrogen-doped TiO_2 with different doping concentrations. The pure TiO_2 sample did not absorb visible light, however, the nitrogen-doped absorption spectrum extended into the visible range of 400 - 500 nm. Furthermore, the absorption strengthened with increasing doping concentration because nitrogen doping contributed to the localized N 2p states in the band structure in the form of substituted and interstitial N states.[21,22]

Figure 4 shows the photocurrent-voltage performances of the films that were undoped and doped with nitrogen at a ratio of N/Ti = 15. The photoelectrochemical response was measured under light on/off illumination in order to confirm whether the photocurrent was specifically generated by only the absorbed photons without any dark current component.

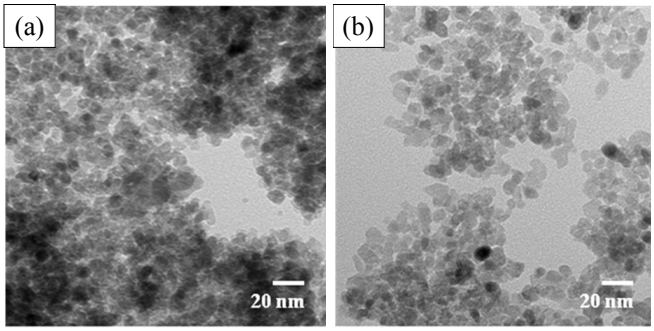

Figure 2. TEM images of (a) pure TiO_2 and (b) nitrogen-doped TiO_2 (N/Ti = 15).

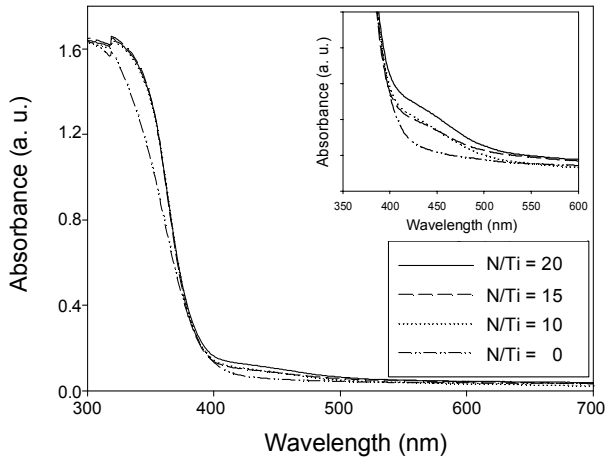

Figure 3. UV-vis diffuse reflectance spectra of nitrogen-doped TiO_2 with various N/Ti ratios.

The dark current under light-off conditions hardly changed across the potential range compared to the photoresponse under light-on conditions. Therefore, the photocurrents of the TiO_2 and TiO_2:N films were generated only by the absorbed photons under light illumination without any contributions from the dark current. For comparison, the PEC response was also measured for a widely used TiO_2 electrode composed of P25 powders. The TiO_2 film synthesized in this study exhibited a superior PEC performance compared to the P25 TiO_2 electrode. Previous reports have shown that P25 is composed of a mixture of anatase and rutile TiO_2 and has a BET of around 65 - 70 m^2/g. On the contrary, the synthesized TiO_2 exhibited only an anatase phase, and its BET surface area was much higher than P25. Therefore, the improved PEC performance of the synthesized TiO_2 mesoporous film was attributed to the much higher surface area and the strictly anatase structure.

Figure 4 also clearly shows that the N-doped TiO_2 electrode exhibited a much higher PEC response than undoped TiO_2. As shown in Table 1, the BET surface area of TiO_2:N (N/Ti = 15) was slightly higher than undoped TiO_2, indicating that the significantly enhanced PEC performance of TiO_2:N could not be explained by this factor alone. Figure 3 showed that the optical absorption extended into a longer wavelength region (or visible region for 400 to 500 nm) with increasing N content. Therefore,

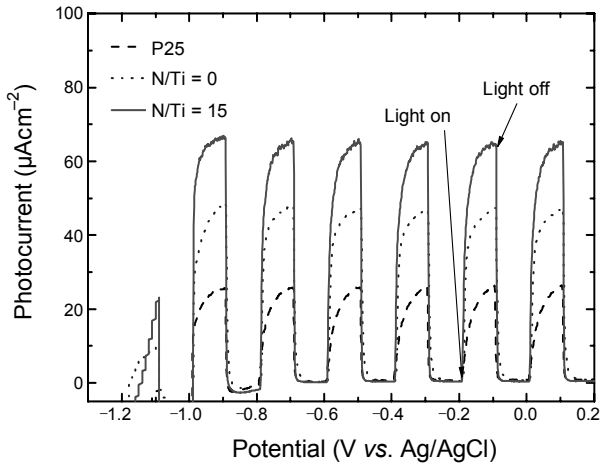

Figure 4. Current-voltage performances of N-doped TiO_2, TiO_2 and P25, respectively, measured under chopped light on/off illumination.

the improved PEC responses of the TiO_2:N films were attributed to the higher visible-photosensitivity as well as the slightly increased surface area because the former increased the photogeneration of the electron-hole pairs, and the later provided a higher number of electrochemical reaction sites. The comparative PEC performance tests were repeated many times to confirm that the results were reproducible.

Conclusions

Nitrogen-doped TiO_2 nanoparticles synthesized by a hydrolysis process were used as photoelectrodes in photoelectrochemical cells for solar water splitting. The samples with a homogeneous anatase phase were easily synthesized through $TiCl_4$ hydrolysis in an ammonia aqueous solution at low temperature. UV-vis DRS spectra depicted the visible light absorption of nitrogen-doped TiO_2, which continued above 500 nm. The TiO_2:N mesoporous electrode exhibited a much higher PEC performance than those of the undoped TiO_2 and P25 electrodes because of its visible-photoresponsibility and slightly increased surface area.

Acknowledgments. This research was supported by the Yeungnam University research grant (209-A-054-030) for the PEC application.

References

1. Fujishima, A.; Honda, K. *Nature* **1972**, *238*, 37.
2. Asahi, R.; Morikawa, T.; Ohwaki, T.; Aoki, K.; Taga, Y. *Science* **2001**, *293*, 269.
3. O'Regan, B.; Grätzel, M. *Nature* **1991**, *353*, 737.
4. Bendavid, A.; Martin, P. J.; Jamting, A.; Takikawa, H. *Thin Solid Films* **1999**, *355*, 6.
5. Lindgren, T.; Mwabora, J. M.; Avendaño, E.; Jonsson, J.; Hoel, A.; Granqvist, C. G.; Lindquist, S. E. *J. Phys. Chem. B* **2003**, *107*, 5709.
6. Yamashita, H.; Ichihashi, Y.; Takeuchi, M.; Kishiguchi, S.; Anpo, M. *J. Synchrotron Rad.* **1999**, *6*, 451.
7. Anpo, M.; Takeuchi, M. *Int. J. Photoenergy* **2001**, *3*, 89.
8. Borgarello, E.; Kiwi, J.; Grätzel, M.; Pelizzetti, E. *J. Am. Chem. Soc.* **1982**, *104*, 2996.

9. Zhao, W.; Ma, W. H.; Chen, C. C.; Zhao, J. C.; Shuai, Z. G. *J. Am. Chem. Soc.* **2004**, *126*, 4782.
10. Ren, W. J.; Ai, Z. H.; Jia, F. L.; Zhang, L. Z.; Fan, X. X.; Zou, Z. G. *Appl. Catal. B: Environ.* **2007**, *69*, 138.
11. Yu, J. G.; Zhou, M. H.; Cheng, B.; Zhao, X. J. *J. Mol. Catal. A: Chem.* **2006**, *246*, 176.
12. Li, D.; Haneda, H.; Labhsetwar, N. K.; Hishita, S.; Ohashi, N. *Chem. Phys. Lett.* **2005**, *401*, 579.
13. Sato, S. *Chem. Phys. Lett.* **1986**, *123*, 126.
14. Asahi, R.; Morikawa, T.; Ohwaki, T.; Aoki, K.; Taga, Y. *Science* **2001**, *293*, 269.
15. Irie, H.; Watanabe, Y.; Hashimoto, K. *J. Phys. Chem. B* **2003**, *107*, 5483.
16. Kitano, M.; Funatsu, K.; Matsuoka, M.; Ueshima, M.; Anpo, M. *J. Phys. Chem. B* **2006**, *110*, 25266.
17. Reyes-Garcia, E. A.; Sun, Y.; Reyes-Gil , K.; Raftery, D. *J. Phys. Chem. C* **2007**, *111*, 2738.
18. Burda, C.; Lou, Y. B.; Chen, X. B.; Samia, A. C. S.; Stout, J.; Gole, J. L. *Nano Lett.* **2003**, *3*, 1049.
19. Zhang, Q.; Gao, L.; Guo, J. *J. Eur. Ceram. Soc.* **2000**, *20*, 2153.
20. Harris, M. T.; Brunson, R. R.; Byers, C. H. *J. Non-Cryst. Solids* **1990**, *121*, 397.
21. Li, H.; Li, J.; Huo, Y. *J. Phys. Chem. B* **2006**, *110*, 1559.
22. Valentin, C. D.; Finazzi, E.; Pacchioni, G.; Selloni, A.; Livraghi, S.; Paganini M. C.; Giamello, E. *Chem. Phys.* **2007**, *339*, 44.